

# Experimental study of strain accumulation of silica sand in a cyclic triaxial test

J. Benoot

KU Leuven @Kulab, Department of Civil Engineering, Zeedijk 101, B-8400 Oostende, Belgium

W. Haegeman

Ghent University, Department of Civil Engineering, Technologiepark 905, B-9052 Zwijnaarde, Belgium

S. François

KU Leuven, Department of Civil Engineering, Kasteelpark Arenberg 40, B-3001 Leuven, Belgium

G. Degrande

KU Leuven, Department of Civil Engineering, Kasteelpark Arenberg 40, B-3001 Leuven, Belgium

**ABSTRACT:** The experimental and phenomenological investigation of the elasto-plastic long-term behaviour of soils under dynamic loading is important for the development of risk analysis tools and numerical accumulation models for settlement prediction. Soil parameters, test equipment and loading conditions have a significant influence on strain accumulation, therefore a parameterization of the silica sand and a description of the re-engineered cyclic triaxial test device are performed in this paper. Long term cyclic triaxial tests are performed on a silica sand to investigate the influence of the number of cycles, the initial void ratio, the mean pressure and packages of cycles on the accumulation of residual strains. Empirical formulations of existing strain accumulation models are validated with test results on dry test samples.

**KEYWORDS:** Cyclic triaxial tests; silica sand; strain accumulation; low level vibrations

## 1 INTRODUCTION

Over the last years the study of soil behaviour under dynamic loading is a growing research domain within the international geotechnical world. This is, amongst others, because of a growing awareness for environment and comfort where vibrations are less tolerated. Repeated small amplitude dynamic loading of soil materials may lead to differential foundation settlements and/or severe damage to structures. Sources of dynamic loadings in the build environment could be pile driving, tunneling, road traffic, trains, et cetera. Karg (2008) demonstrated that single or only a few loading events show no residual deformations in soil. However, after a large number of events, residual deformation is observable in many cases. This phenomenon – (almost) elastic behaviour in the short term, but non-negligible plastic behaviour over a large number of vibrations – is called strain accumulation.

## 2 THEORETICAL BACKGROUND

Triaxial tests are performed in axisymmetric test conditions ( $\sigma'_2 = \sigma'_3$ ). The stresses are applied in axial and lateral direction alone (figure 2.1). The effective lateral stress  $\sigma'_3 = \sigma_c - u$  with  $\sigma_c$  the cell pressure and  $u$  the pore pressure. The effective axial stress  $\sigma'_1$  is determined by the cell pressure, the constant axial stress  $\sigma_a$  and a cyclic stress with amplitude  $\sigma_1^{ampl}$ :  $\sigma'_1 = \sigma_c + \sigma_a - u \pm \sigma_1^{ampl}$ .

The stress invariants for axisymmetric test conditions are:

$$p' = \frac{\sigma'_1 + 2 \cdot \sigma'_3}{3}, \quad q = \sigma'_1 - \sigma'_3 \quad (1)$$

For axisymmetric test conditions the earth pressure coefficient  $K = \sigma'_3 / \sigma'_1$ .

A similar parameter to express the stress state in a  $p'$ - $q$  plane is  $\eta$ , defined by:

$$\eta = \frac{3(1 - K_0)}{1 + 2K_0} \quad (2)$$

All tests in this paper are performed on completely dry samples. This means that the pore water pressure  $u$  is zero and all total stresses are equal to the effective stresses. In all tests the

average stress was kept constant and the axial stress cyclically varied with an amplitude  $\sigma_1^{ampl}$  (figure 2.1). The normalized stress amplitude is defined as:

$$\zeta = \frac{\sigma_1^{ampl}}{p'} \quad (3)$$

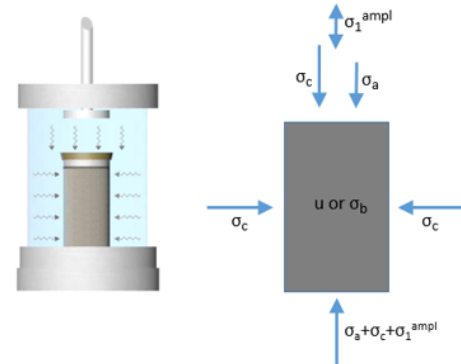


Figure 2-1: Stress conditions cyclic triaxial cell

A typical stress path is defined in figure 2.2. First stages are the isotropic and optional anisotropic loading stages until  $(p^{av}, q^{av})$  is reached, followed by the cyclic loading stage.

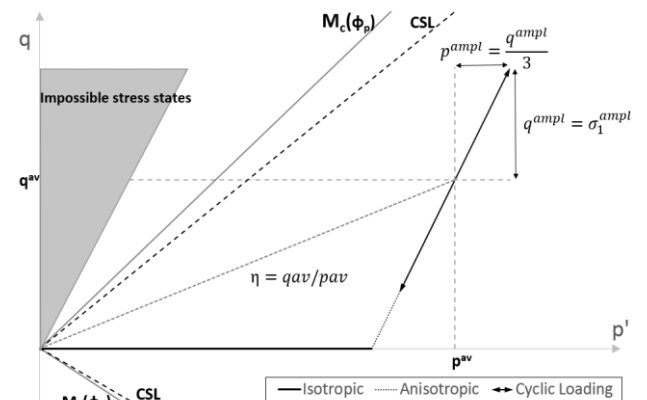


Figure 2-2: Cyclic stress path in the  $p'$ - $q$  plane

By analogy with the stresses, the axisymmetric test conditions result in a simplification for the strains as well. In axisymmetric conditions the two lateral strains are equal ( $\varepsilon_2 = \varepsilon_3$ ) and the strain invariants are equal to:

$$\begin{aligned}\varepsilon_p &= \varepsilon_1 + 2\varepsilon_3 \\ \varepsilon_q &= \frac{2}{3}(\varepsilon_1 - \varepsilon_3)\end{aligned}\quad (4)$$

where  $\varepsilon_1$  and  $\varepsilon_3$  denote the principal strains in axial and lateral direction, respectively. Alternatively, the deviatoric strain is denoted as  $\gamma = \varepsilon_1 - \varepsilon_3$ . In the case of long-term cyclic loading the total strain  $\varepsilon$  is the sum of an accumulated, residual portion  $\varepsilon^{acc}$  and an elastic, resilient portion  $\varepsilon^{ampl}$ :

$$\varepsilon = \varepsilon^{ampl} + \varepsilon^{acc} \quad (5)$$

### 3 TEST DEVICE

#### 3.1 Original test device

The cyclic triaxial system applies cyclic or dynamic loading to a cylindrical soil specimen. Two models of triaxial cells for specimen sizes of 50 mm and 100 mm in diameter are available. The system is a digitally controlled, servo-pneumatic system which controls three parameters: axial stress, confining pressure and back pressure. Within the servo-pneumatic testing system, energy is transmitted to the specimen using high pressure air acting on a double sided piston (actuator). The total system works on a filtered clean air supply with a minimum pressure of 800 kPa.

Demineralised water is used to saturate the sample in the case of saturated samples and to fill the triaxial cell. The supplied air pressure is transformed to water pressure using two bladders, one for back and one for cell pressure, respectively.

A conventional triaxial loading frame including separate manual assessable monotonic shearing device is upgraded with an actuator crosshead carrying the pneumatic actuator for axial cyclic loading. A double acting digitally controlled pneumatic actuator with a range of  $\pm 5$  kN applies the axial (cyclic or monotonic) load. The submersible  $\pm 5$  kN load cell measures the applied load above the top cap. The actuator requires a minimum air supply of 800 kPa, which corresponds with the air supply of the total pneumatic system. Cyclic and monotonic loading can be load [kN], stress [kPa], displacement [mm] or strain [%] controlled. Possible cyclic loadings are sinusoidal, triangle, saw-tooth, ... and a user defined cyclic load. The cyclic triaxial system is designed to perform the following tests: saturation, isotropic and anisotropic consolidation, standard triaxial tests (CD, CU, UU), user defined cyclic loading, investigation of liquefaction potential (ASTM D5311), determination of E, G and D (ASTM 3999-91).

During the tests, there is a possibility to measure ten transducers at the same time. The first three readings are those from the controlled pressures: cell, back and axial pressure. Further there is a possibility to measure pore water pressure and the volume change. In addition axial movements are measured by the actuator and external linear displacement meters. Both have a range of  $\pm 15$  mm and  $\pm 25$  mm respectively.

#### 3.2 Test procedure

All test samples are approximately 190 mm in height and 100 mm in diameter. This results in a height-to-diameter ratio (H/D) of 1.9 which is a little less than the recommended ratio according to ASTM D 3999-91 (H/D  $\approx 2$  à 2.5). The chosen lower height of the test samples is related to the dimensions of the triaxial cell and to obtain enough space for axial movements of the load cell. All tests are performed on reconstituted dry specimens. Therefore the moist tamping with undercompaction method, first proposed by Ladd (1978), is used. The consolidation phase with dry test samples is much different from the consolidation phase with saturated test samples. In the case of dry test samples there is no back pressure ( $\sigma_b = 0$  kPa).

In a first step, the consolidation phase is always performed isotropically and there is a possibility for anisotropic consolidation in a second step depending on the requested test specification. Starting the consolidation occurs with the specimens drainage valves closed, increasing the cell pressure until it equals the desired effective consolidation stress ( $\sigma_b = 0$  kPa). For anisotropic consolidation an additional axial stress  $\sigma_a$  is applied to the specimen. Since completely dry samples are tested, no confining pressure is transferred to the pore water and there is no increase of the pore pressure. This is a common way to apply the desired effective stresses.

As a specimen is loaded under the requested stress conditions, cyclic loading can be applied. The current equipment allows for a wide range of predefined axial cyclic loading options. In this research only the user defined option for the long term tests is used.

#### 3.3 Re-engineering the CDAS and software step-up

Previous research indicated some shortcomings related to the test equipment. Therefore it was decided to modify the equipment extensively. A first limitation of the original test equipment is the test frequency of the cyclic loading. According to the manufacturer, the electrically controlled pneumatic servo valve coupled to the actuator has a response typically better than 70 Hz. Karg (2008) concluded already that there was a problem with the data acquisition and the performance of the actuator at frequencies above 10 Hz. For this reason, together with the fact that the current CDAS operates as a complete black box, it was chosen to install a complete new data acquisition system from National Instruments. This new acquisition system is a combined PXI-1050 chassis that integrates a high-performance 8-slot PXI subsystem with a 4-slot SCXI subsystem. All sensors are connected, through a switch panel, to the PXI-1050.

Besides the new data acquisition system, the software undergoes numerous modifications as well. The old software was user friendly and had extensive opportunities, but also some limitations such as the protected code. In that way it wasn't possible to program new test specifications. The new software, created in Labview, will have the same possibilities as the old one, with 3 concrete expansions

First, the consolidation procedure will be modified. It is known that failure stresses in soils are dependent on the stress history. With the old software, there was only an isotropic and anisotropic consolidation executable. The stress paths therefore are respectively:

$$\frac{q'}{p} = 0, \quad \frac{q'}{p} = 3 \quad (6)$$

Next to isotropic and anisotropic consolidation, there will be an opportunity for  $K_0$  consolidation in the new software. In a  $K_0$  consolidation process, the diameter remains constant ( $\Delta \varepsilon_r = 0$ ) and the slope of the effective stress path becomes:

$$\frac{q'}{p} = \frac{3 * (1 - K_0)}{1 + 2 * K_0} \quad (7)$$

Second modification is to include the bender element tests. Until now the bender element test equipment is installed completely separate from the cyclic triaxial control and data acquisition. The signal is generated by the soundcard of the PC that controls the CDAS. The new triaxial and bender element software will be combined in one program. That way, there is no need for an external PC oscilloscope.

Third modification is related to the cyclic loading. Until now, there is a possibility to generate sinusoidal, triangular or other predefined cyclic waves. In the new software there will be, next to the predefined waves, a possibility to generate random cyclic waves. These random waves will be analyzed by the rainflow counting algorithm. In that way, there is a possibility to analyse the difference between complete random loading and packages of cycles.

#### 4 TEST MATERIAL

All tests analysed during this research are performed on a uniform fine grained sand of Mol. Figure 4.1 shows the grain size distribution curve of the tested material. The mean grain size diameter is  $d_{50}=0.167$ , the uniformity coefficient  $C_u=1.49$  and the coefficient of curvature  $C_c=0.87$ . The density of the soil particles ( $\rho_p$ ) is  $2610 \text{ kg/m}^3$ ,  $e_{\max}=0.918$  and  $e_{\min}=0.586$ .

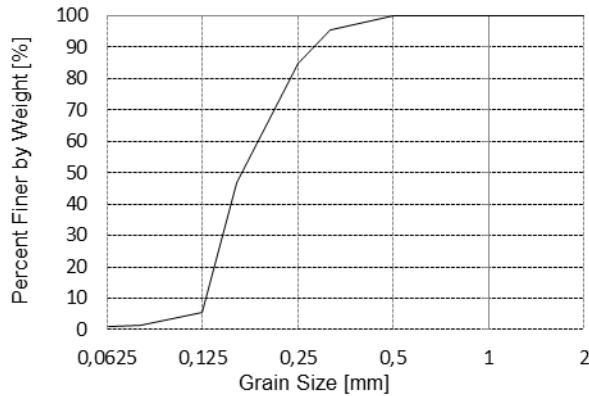


Figure 4-1: Grain size distribution curve of the sand of Mol

#### 5 TEST RESULTS

##### 5.1 Strain accumulation with the number of cycles

Dynamic or cyclic loading results in stress-strain hysteresis loops. One small amplitude load cycle is almost a perfectly closed hysteresis loop. So, the elastic behaviour of the sand can be stated for every single load cycle, independently of the cycle number. However, analysis of a large number of load cycles (for instance 100000 cycles), demonstrate that residual deformations take place. Figure 5.1 demonstrates clearly the movement of the hysteresis loops between the first and 100000<sup>th</sup> loading cycle.

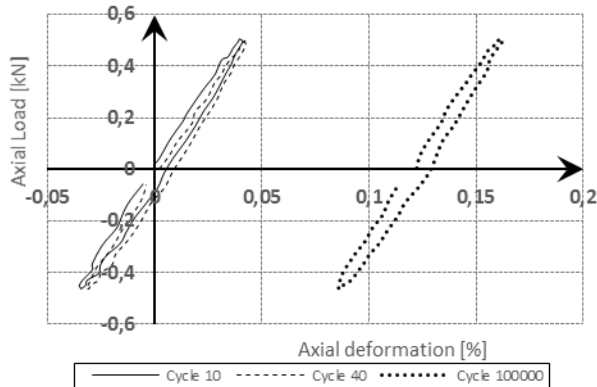


Figure 5-1: Movement of hysteresis loops

##### 5.2 Influence of the initial void ratio

Long-term cyclic triaxial tests are performed on dry samples with identical size and prepared in accordance with the procedure of Ladd. The samples are pressurized with an effective mean pressure of  $p' = 200 \text{ kPa}$  and  $K = 0.9$ . The cyclic loading stage is performed with user defined loading parameters. 100000 cycles are applied with a peak to peak amplitude of  $\sigma_1^{pp} = 120 \text{ kPa}$ . Three tests are performed with different initial void ratios ( $e_0=0.817$ ,  $0.770$  and  $0.705$ ) to determine the influence on the accumulation rate. Fig 5.2 shows the accumulated axial strain as a function of the number of load cycles. Higher initial void ratios obviously lead to higher accumulation of residual strains. Performing tests at different relative densities results in different strain amplitudes  $\varepsilon^{\text{ampl}}$ . In order to achieve comparability all curves are normalized using the functions:

$$f_{\text{ampl}} = \begin{cases} \left( \frac{\varepsilon^{\text{ampl}}}{\varepsilon^{\text{ref}}} \right)^2 & \text{for } \varepsilon^{\text{ampl}} \leq 10^{-3} \\ 100 & \text{for } \varepsilon^{\text{ampl}} > 10^{-3} \end{cases} \quad (8)$$

$$f_e = \frac{(C_e - e)^2}{1 + e} \frac{1 + e_{\text{ref}}}{(C_e - e_{\text{ref}})^2} \quad (9)$$

Both formulations are proposed by Wichtmann (2005). Equation (8) describes the influence of  $\varepsilon^{\text{ampl}}$  on the strain accumulation rate with  $\varepsilon_{\text{ref}}^{\text{ampl}}=10^{-4}$ . Equation (9) describes the influence of the initial void ratio on strain accumulation.

To validate the proposed equations (8) and (9) of Wichtmann, all curves of figure 5.2 are divided by  $f_{\text{ampl}}$  and  $f_e$ . For  $e_{\text{ref}}=e_{\max}=0.918$  and the material parameter  $C_e=0.45$  all curves fall closely together when normalized with the functions  $f_{\text{ampl}}$  and  $f_e$  (Figure 5.3). Consequently, the presented test results coincide with the conclusions of Wichtmann and confirm the usefulness of the  $f_{\text{ampl}}$  and  $f_e$  for accumulated axial strain on dry test samples.

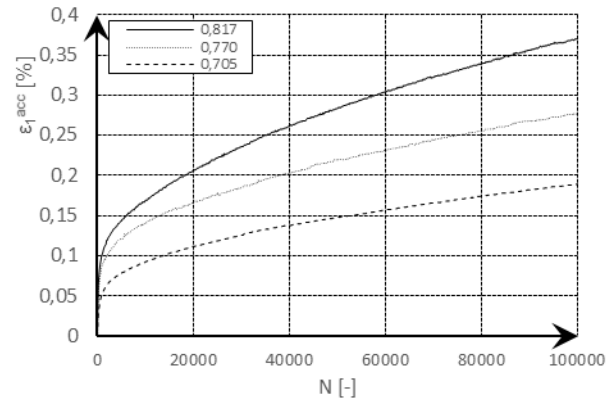


Figure 5-2: Residual axial strain as a function of N in tests with different  $e_0$

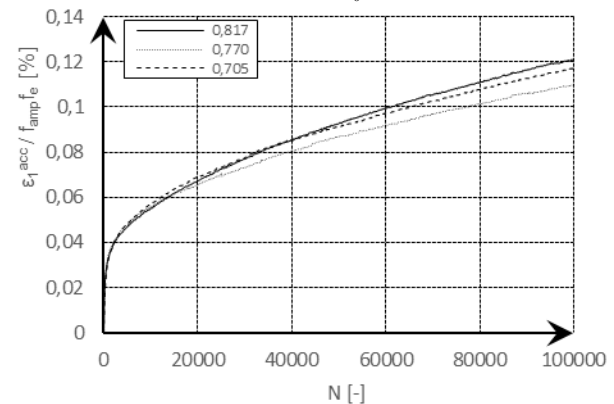


Figure 5-3: Normalized residual axial strain as a function of N in tests with different  $e_0$

##### 5.3 Influence of the mean effective stress $p'$

Long-term cyclic triaxial tests are performed on dry samples with identical size and prepared in accordance with the procedure of Ladd. All samples have an initial relative density of approximately 60%, corresponding to an initial void ratio of approximately 0.72 (range:  $0.7177 < e_0 < 0.7234$ ). The cyclic loading stage is performed under user defined conditions. 100000 load cycles are applied at a loading frequency of 2 Hz and a peak to peak amplitude of 40 kPa. Different confining pressures ( $p'=15, 30, 60$  and  $100 \text{ kPa}$ ) are chosen to determine the influence on the axial accumulation rate. Figure 5.4 shows the accumulated axial strain as a function of the number of load cycles. Lower mean effective stress leads to higher accumulation of residual strains.

In order to achieve comparability all curves are normalized using the following function:

$$f_p = \exp \left[ -C_p \left( \frac{p'}{p_{ref}} - 1 \right) \right] \quad (10)$$

This formulation is proposed by Wichtmann (2005), describing the influence of  $p'$  on the strain accumulation rate, with  $p_{ref} = 100$  kPa,  $e_{ref} = e_{max}$  and  $C_p$  is a material constant

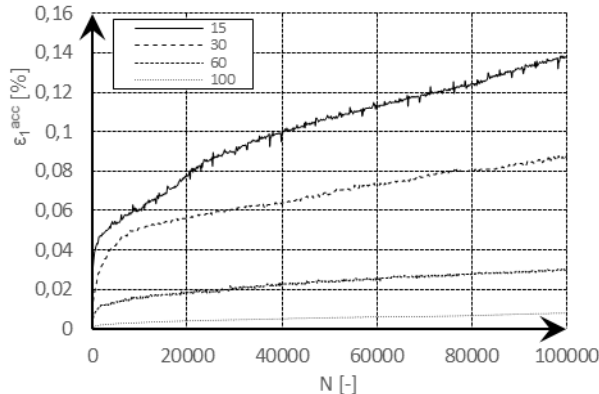


Figure 5-4: Residual axial strain as a function of N in tests with different  $p'$

As for the material parameter  $C_p = 3.45$  all curves fall closely together when normalized with function  $f_p$  as shown in figure 5.5. Presented test results coincide with conclusions of Wichtmann and confirm the usefulness of equation (10) for accumulated axial strain on dry test samples.

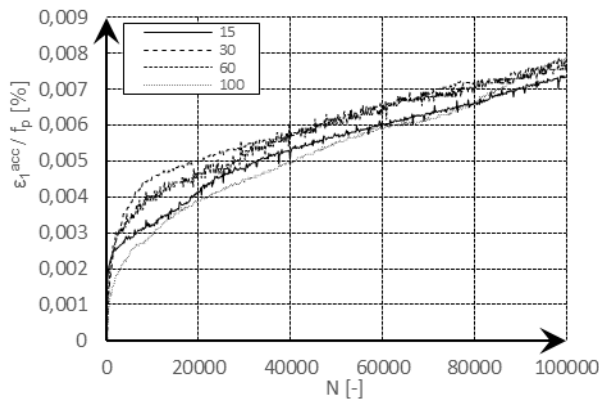


Figure 5-5: Normalized residual axial strain as a function of N in tests with different  $p'$

#### 5.4 Packages of cycles

In many practical problems (traffic loads, earthquakes, wind, waves,...), the amplitude of the loading cycles is not constant but varies from cycle to cycle. Such random cyclic loadings cannot be calculated with an explicit accumulation model since  $\epsilon^{ampl}$  has to be a constant during a specific number of cycles. The most widely used procedure for determining the equivalent number of uniform stress cycles is based on the hypothesis of Miner for metals. By means of stochastic methods (e.g. rain flow counting), an irregular cyclic loading can be replaced by packages of cycles with a constant amplitude. The question arises, if the sequence of the packages influences the final value of the residual strain.

Two cyclic triaxial tests are performed with an effective mean pressure of  $p=150$  kPa and  $K=0.8$ . The cyclic loading stage is performed with user defined loading parameters, 40000 loading cycles are applied with a sinusoidal waveshape. Four packages each with 10000 cycles were applied in succession for each test. The first test is performed with  $\sigma_1^{PP} = 10;20;40;60$  kPa and the second one with  $\sigma_1^{PP} = 60;40;20;10$  kPa (Figure 5.6). It is clearly seen that the hypothesis of Miner is also valid for this sand, since the residual strain in both tests is equal.

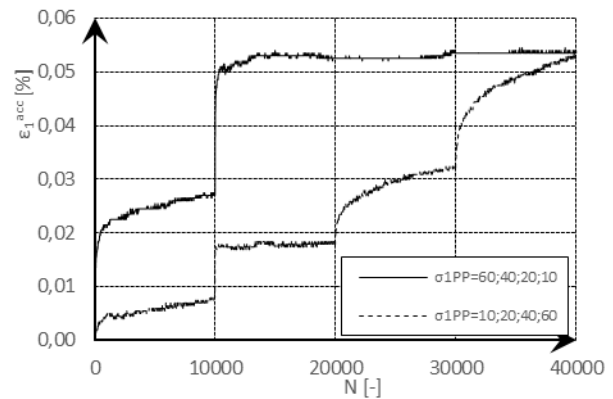


Figure 5-6: Residual axial strain as a function of N in tests with packages of cycles

## 6 CONCLUSIONS

Long term cyclic triaxial tests are performed on a fine graded sand of Mol to investigate the influence of the number of cycles, the initial void ratio, the mean pressure  $p'$  and packages of cycles on the accumulation of residual strains. The empirical formulations proposed by Wichtmann, namely the amplitude function  $f_{ampl}$ , void ratio function  $f_e$  and mean pressure function  $f_p$ , are validated with own test results on dry samples and a higher strain level. For the performed tests, all curves fall closely together when normalized with the correct empirical function. Consequently, the presented test results coincide with the conclusions of Wichtmann and confirm the usefulness of the empirical formulations for accumulated axial strain on dry test samples.

If the soil is loaded by packages of cycles with different amplitudes, the sequence of the packages plays a minor role concerning the residual strain at the end of the test. Thus, Miner's rule is applicable to sand subjected to cyclic loadings.

Development of the CDAS and software re-engineering is in progress.  $K_0$  consolidation and the rainflow counting algorithm will be in operation in the near future. In that way, it will be possible to apply random cyclic loading cycles and to determine the equivalent cyclic amplitude values (packages of cycles).

## 7 REFERENCES

- ASTM E 1049-45. (2011). *Standard practices for cycle counting in fatigue analysis*.
- Francois, S., Franken, P., Degrande, G., & Haegeman, W., Long term accumulation of deformation in granular soils under multi-axial cyclic loading. *Proceedings of the 15th European Conference on Soil Mechanics and Geotechnical Engineering*, 541-544, Athens, 2011.
- Kaggwa, W. S., Booker, J. R., & Carter, J. P. (1991). Residual strains in calcareous sand due to irregular cyclic loading. *Journal of geotechnical engineering, ASCE*, (117(2)), 201-218,1991.
- Karg, C. (2008). *Modelling of Strain Accumulation Due to Low Level Vibrations in Granular Soils*. Ghent University, PhD.
- Ladd, R. (March 1978). Preparing test specimens using undercompaction. *Geotechnical Testing Journal*, Vol. 1, No. 1, 16-23.
- Lentz, R. W., & Baladi, G. Y. (January 1980). Simplified procedure to characterize permanent strain in sand subjected to cyclic loading. *International symposium on soils under cyclic and transient loading*, (pp. 89-95), January 1980.
- Travis, J., & Kring, J. (2009). *Labview For Everyone: Graphical Programming Made Easy and Fun*. Pearson Education.
- Verruijt, A. (2010). *An introduction to soil dynamics*. TU Delft: Springer.
- Wichtmann, T. (2005). *Explicit accumulation model for non-cohesive soils under cyclic loading*. Ruhr Universität Bochum, PhD, Germany.